Controlling the Motion of Magnetic Flux Quanta

B. Y. Zhu,[1] F. Marchesoni,[1,2,*] and Franco Nori[1,3,*]

[1]*Frontier Research System, The Institute of Physical and Chemical Research (RIKEN), Wako-shi, Saitama 351-0198, Japan*
[2]*Istituto Nazionale di Fisica della Materia, Universitá di Camerino, I-62032 Camerino, Italy*
[3]*Center for Theoretical Physics, Physics Department, University of Michigan, Ann Arbor, Michigan 48109, USA*

(Received 3 May 2003; published 6 May 2004)

We study the transport of vortices in superconductors with triangular arrays of boomerang- or V-shaped asymmetric pinning wells, when applying an alternating electrical current. The asymmetry of the pinning landscape induces a very efficient "diode" effect, that allows the sculpting at will of the magnetic field profile inside the sample. We present the first quantitative study of magnetic "lensing" of fluxons inside superconductors. Our proposed vortex lens provides a near threefold increase of the vortex density at its "focus" regions. The main numerical features have been derived analytically.

DOI: 10.1103/PhysRevLett.92.180602 PACS numbers: 05.40.–a

Driven by nonequilibrium fluctuations, biological motors are examples of stochastic devices that bias the Brownian motion of particles in an anisotropic medium (see, e.g., [1,2]). These motors are inspiring novel solid-state devices [3] that allow controlling the motion of small "particles," including electrons, colloidal particles, and magnetic flux quanta. Here we consider superconducting devices that are inspired by such molecular motors. In particular, for samples with anisotropic pinning, dc transport of magnetic flux quanta may be driven by an ac current in the absence of noise.

The control of the motion of vortices using asymmetric pinning [4,5] can be useful for applications, including the removal of unwanted trapped flux in devices [6]. Indeed, one of the main problems degrading the performance of superconducting devices is the noise produced by fluctuating trapped magnetic flux. Flux pumps, rectifiers, or diodes [4,5] have been proposed. Indeed, several groups [4,5,7] have studied quite different ways of using potential energy ratchets in superconductors. We present the first quantitative study of *magnetic lensing* or shaping and "sculpting" micromagnetic profiles inside superconductors. For instance, our proposed vortex lens provides a near threefold increase of the vortex density at its focus regions. Our main numerical results have also been derived analytically.

Using molecular dynamics simulations, we study the dynamics of ac-driven vortices subject to the "ratchet effect" of boomerang-shaped asymmetric pinning sites. We observe a net longitudinal transport of the vortices when $H/H_1 > 1$, and a maximum rectification when $H/H_1 \approx 2$. Here H_1 is the field at which the total number of vortices N_v matches the number of pinning sites N_p. Moreover, we obtain a *pronounced lensing effect* at the interface between stripes of boomerang traps with opposite orientation (termed here *bras*, $<$, and *kets*, $>$).

Model.— The plot in the inset of Fig. 1 shows schematically the geometry of the triangular lattice of identical boomerang-shaped pinning centers oriented as kets: $>$. Here, the length s_0 of the two boomerang linear arms is kept fixed, while varying the pinning lattice constant a_0 and the angle α between the arms. The pinning force F_p exerted on each vortex is $\mathbf{F}_p(\mathbf{r}) = -F_{p0} f_0(\mathbf{r}/R_p) \exp(-|\mathbf{r}/R_p|^2)$. Here, $\mathbf{r}$ is the distance between the vortex and the boomerang closest point; R_p and $F_{p0} f_0$ denote the strength and the range of the pinning force, respectively [5,8,9].

The ac square-wave driving Lorentz force is $\mathbf{F}_L = F_L^x(t)\,\hat{\mathbf{x}}$ and the repulsive vortex-vortex interaction is approximated to $\mathbf{F}_{vv}(\mathbf{r}_i) = F_{vv0} f_0 \sum_{j\neq i}^{N_v} \lambda \hat{\mathbf{r}}_{ij}/|\mathbf{r}_i - \mathbf{r}_j|$, where $\hat{\mathbf{r}}_{ij} = (\mathbf{r}_i - \mathbf{r}_j)/|\mathbf{r}_i - \mathbf{r}_j|$ and $F_{vv0} f_0$ denotes its intensity. The overdamped equation of motion [5,8,9] of the ith vortex is $\eta \mathbf{v}_i = \mathbf{F}_L + \mathbf{F}_{vv}(\mathbf{r}_i) + \mathbf{F}_p(\mathbf{r}_i)$. In our simulation this equation is solved (with $\eta = 1$) by taking discrete time steps $\tau_0 = 0.03$ in a 2D sample with periodic boundary conditions. The initial vortex positions are obtained by annealing and then subjected to an alternating current along the y axis, which in turn exerts a square-wave Lorentz driving force along the x axis with amplitude F_L and half period P. For brevity, here we focus on the case $a_0/s_0 = 4$, $\alpha = 2\pi/3$, $R_p = 0.4$, $\lambda = 6$, $s_0 = \lambda/2$, $F_{p0} = 2$, and $F_{vv0} = 0.1$, although very many other parameter values were also simulated.

Net voltage $V_{\rm dc}$ versus ac drive period.— Figure 1(a) shows the stationary time average of the vortex current $V_{\rm dc} = \sum_i^{N_v} v_i/N_v$ for different amplitudes F_L of the ac drive. Each plotted point is obtained by averaging over 100 periods, each with 10^4 to 10^6 time steps, depending on the choice of P (typically, the stationary regime is well established after a relaxation time of $200P$). Interestingly, when increasing the half period of the driving force (from $P = 0$ to $10^4\tau_0$ with very small step $\Delta P = 20\tau_0$), a sharp jump appears in the rectified voltage $V_{\rm dc}(P)$ followed by a sequence of damped oscillations.

The origin of the rectification effect can be explained as follows. When $H/H_1 \leq 1$, the vortex diode effect cannot manifest itself because, the vortex-vortex interaction is weak (for such low fields), and each pinning site has at most one vortex. Thus, the depinning to the left or the right is the same, and the path followed by

each individual vortex is essentially the same in either direction.

The corresponding depinning force is determined through the analytical expression for $\mathbf{F}_p(\mathbf{r})$ irrespective of the $\mathbf{F}_L$ orientation, $F_{\pm}^{\mathrm{depin}}(H/H_1 = 1) \simeq 0.86$. Pinning centers with double occupancy show up as H is being increased above the first matching field H_1. When $\mathbf{F}_L \parallel \mathbf{x}$ both trapped vortices tend to pile up towards the boomerang central cusp of the ket $>$. Because of the strong vortex-vortex repulsion between these two trapped vortices, the minimum force required to extract the first vortex, $F_{+}^{\mathrm{depin}}(H/H_1 = 2) \simeq 0.65$ for $\alpha = 2\pi/3$, is lower than for the single occupancy case. However, if $\mathbf{F}_L \parallel -\mathbf{x}$ two vortices trapped at the same boomerang-shaped pinning well will move towards the two opposite boomerang tips. The distance between two such vortices is then relatively large for their repulsion to favor the depinning mechanism appreciably, hence $F_{-}^{\mathrm{depin}}(H/H_1 = 2) \simeq F_{\pm}^{\mathrm{depin}}(H/H_1 = 1) \simeq 0.86$. [For the sake of comparison, we mention that in the case of triple occupancy the first depinning forces are $F_{+}^{\mathrm{depin}}(H/H_1 = 3) \simeq 0.57$ and $F_{-}^{\mathrm{depin}}(H/H_1 = 3) \simeq 0.65$, respectively]. As a consequence, vortices trapped in the sample move a longer distance during the positive eastbound drive half cycle than during the negative westbound one, and this produces a nontrivial rectified flow of depinned vortices in the $\mathbf{x}$ direction for F_L in the interval (0.65, 0.86).

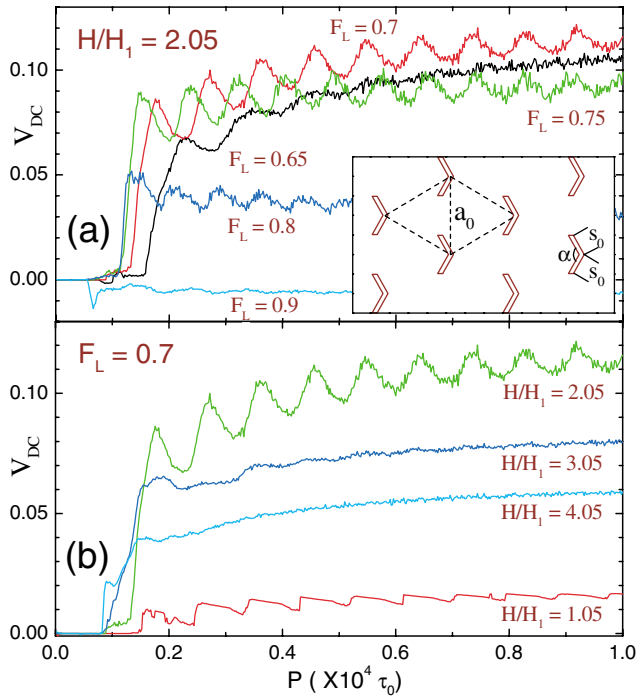

FIG. 1 (color). (a) Average net dc velocity V_{dc} versus the half period P of the ac drive for different amplitudes F_L: $F_L =$ 0.65, 0.7, 0.75, 0.8, and 0.9 with $H/H_1 = 2.05$ and $N_p = 120$. (b) V_{dc} versus P for different ratios of vortices to pins, i.e., $H/H_1 = 1.05$, 2.05, 3.05, and 4.05, with fixed amplitude of the drive force $F_L = 0.7$, and $N_p = 120$. The inset in (a) shows a unit cell of the triangular lattice of boomerang-shaped pinning traps oriented as kets $>$; the bisector of the angle α of each trap is always along the x axis.

In the absence of both thermal and pinning forces, a single vortex would alternate traveling a distance $F_L \times P$ in the $\mathbf{x}$ direction and then a distance $F_L \times P$ in the opposite $-\mathbf{x}$ direction. Thus, the minimum half period P_c for the driving force F_L to induce a substantial vortex current is of the order of $P_c \sim a_0\sqrt{3}/F_L$, i.e., the time a vortex takes to advance the entire distance between two adjacent pinning sites sitting on the same bisector. This is the reason why the onset of the $V_{\mathrm{dc}}(P)$ curves in Fig. 1(a) clearly depends on F_L. The *oscillation* of $V_{\mathrm{dc}}(P)$ for $P > P_c$ and $1 < H/H_1 < 3$, is another remarkable feature of this asymmetric system. The period of these oscillations coincides with P_c itself, as on increasing the forcing half period P by an amount P_c, the depinned vortices succeed in reaching one trapping boomerang farther in the $\mathbf{x}$ direction before the drive reverses its sign; this optimizes the rectification mechanism as a function of the ac drive frequency. Interestingly, when $F_L = 0.9$, i.e., for $F_L > F_{\pm}^{\mathrm{depin}}(H/H_1 = 1)$, we obtain a very weak negative dc response (vortex current *inversion*).

The density of the vortices in the sample also plays an important role in determining the intensity of their dc response to an external ac drive, as shown in Fig. 1(b). In the low density regime, $H/H_1 \lesssim 1$, each pinning center can trap at most one vortex, so for $F_L = 0.7$ all vortices stay pinned, being $F_L < F_{\pm}^{\mathrm{depin}}(H/H_1 = 1) \simeq 0.86$. At higher densities, $H/H_1 > 1$, pinning centers can trap more than one vortex. Let us now consider $F_L = 0.7$, which falls between the two pinning forces $F_{+}^{\mathrm{depin}}(H/H_1 = 2) \simeq 0.65$ and $F_{-}^{\mathrm{depin}}(H/H_1 = 2) \simeq 0.86$. For this value of F_L the applied ac drive suffices to strip each pinning site of all its vortices besides either one (that remains trapped when $\mathbf{F}_L \parallel \mathbf{x}$), or two (that remain pinned when $\mathbf{F}_L \parallel -\mathbf{x}$). Therefore at most one vortex per pinning site

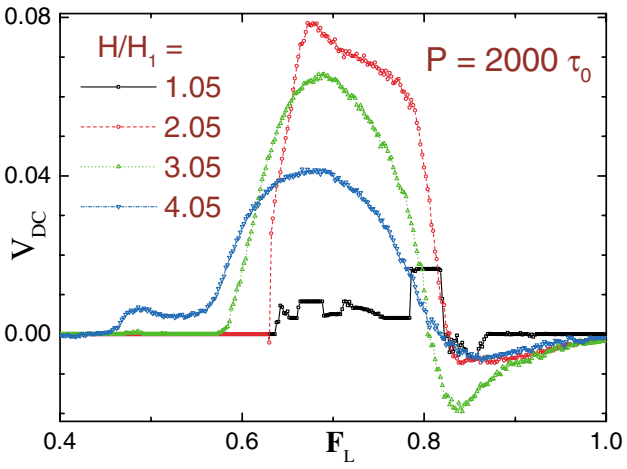

FIG. 2 (color). Net average dc velocity V_{dc} versus amplitude F_L of the ac driving force for various magnetic fields $H/H_1 =$ 1.05, 2.05, 3.05, and 4.05, with fixed half period $P = 2000\tau_0$. The side peaks at $H/H_1 = 3.05$ and 4.05 signal a re-entrant vortex current involving unpinned vortices at zero bias [10].

actually participates in the rectification mechanism, and V_{dc} is always positive. Therefore, the asymptotic values of the $V_{dc}(P)$ curves displayed in Fig. 1(b) are expected to scale like $H_1/2H$ for $H/H_1 > 2$ and $1 - H_1/H$ for $H/H_1 \leq 2$, in good agreement with our simulation. This can be seen, e.g., via $V_{dc} = \sum_i^{N_v} v_i/N_v \sim V_{aver}/H \sim (v_+ + v_-)/2H \sim v_+/2H \sim 1/2H$, since $N_v \sim H$, $V_{aver} \sim (v_+ + v_-)/2$, $v_- \sim 0$, and $v_+ \sim 1$. For lower fields, $H/H_1 \leq 2$, the dependence $1 - H_1/H$ satisfies the constraint $V_{dc}(H = H_1) = 1 - H_1/H_1 = 0$. The scaling relations above explain why, on raising H/H_1 above 2, the relevant net velocities V_{dc} grow weaker, as shown in Figs. 1 and 2. Notice that increasing the number of interstitially flowing vortices also suppresses the V_{dc} oscillations of Fig. 1, as mutually repelling unpinned vortices are less sensitive to the pinning-depinning mechanism.

Net dc voltage versus amplitude.—Figure 2 shows the optimal ac drive amplitude for the dc response of the system at different values of H/H_1 and constant $P = 2000\tau_0$. It is clear that when F_L is smaller than a certain threshold, none of the trapped vortices can be depinned and no dc response is observed. The amplitude F_L that maximizes the dc response depends on the ratio H/H_1. For $H/H_1 = 1.05$, only the interstitial vortices, about 5% of the total, are rectified. The very small scale fluctuations in $V_{dc}(F_L)$ are due to discommensurations [9] between the vortices and pinning centers, and to the geometry of the pinning sites.

For higher magnetic fields, e.g., $H/H_1 = 2.05$, 3.05 and 4.05, the curves $V_{dc}(F_L)$ exhibit a well defined maximum in the range $[\, F_+^{depin}(H/H_1 = 2),\ F_-^{depin}(H/H_1 = 2)\,]$, i.e., $[0.65, 0.86]$. On raising the vortex density, the onset of the vortex current shifts towards lower F_L values, since the lowest depinning forces F_+^{depin} decrease with increasing H/H_1. Most remarkably, as F_L grows larger than the largest depinning force, $F_L \gtrsim F_\pm^{depin}(H/H_1 = 1) \simeq 0.86$, V_{dc} becomes negative, no matter what the value of H/H_1 (Fig. 2) and P [Fig. 1(a), $F_L = 0.9$]. The reason is that for $\mathbf{F}_L \parallel \mathbf{x}$ movable vortices flow forward along the bisector of each boomerang row, while for $\mathbf{F}_L \parallel -\mathbf{x}$ they move backwards through the interstitial channels delimited by each pair of adjacent boomerang rows. Traversing the pinning sites ($\mathbf{F}_L \parallel +\mathbf{x}$) hinders the free motion of the

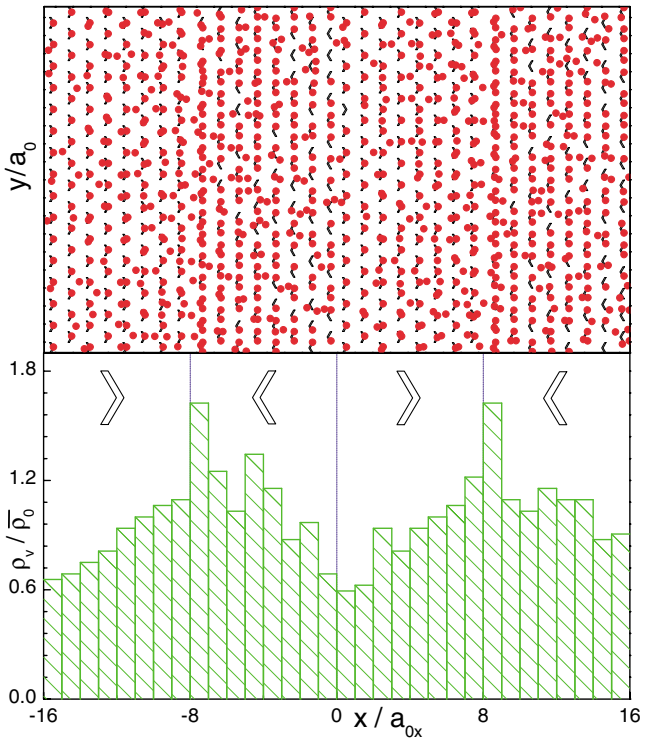

FIG. 3 (color). Top panel: top view of the boomerang array (black *bras* $<$ and *kets* $>$) with driven vortices (red dots) after a sequence of 50 ac cycles with $F_L = 0.7$ and $P = 2000\tau_0$. Lower panel: vortex density $\rho_v(x)/\bar{\rho}_0$ versus position along the x axis. Here, $a_{0x} = a_0 \sin(\alpha/2)$, $\bar{\rho}_0 \equiv H/H_1 = 2$, and $N_p = 128 \times 4 = 512$. All remaining pinning site parameters are as in Fig. 1. This snapshot shows an increase in ρ of about 3 from its minimum value.

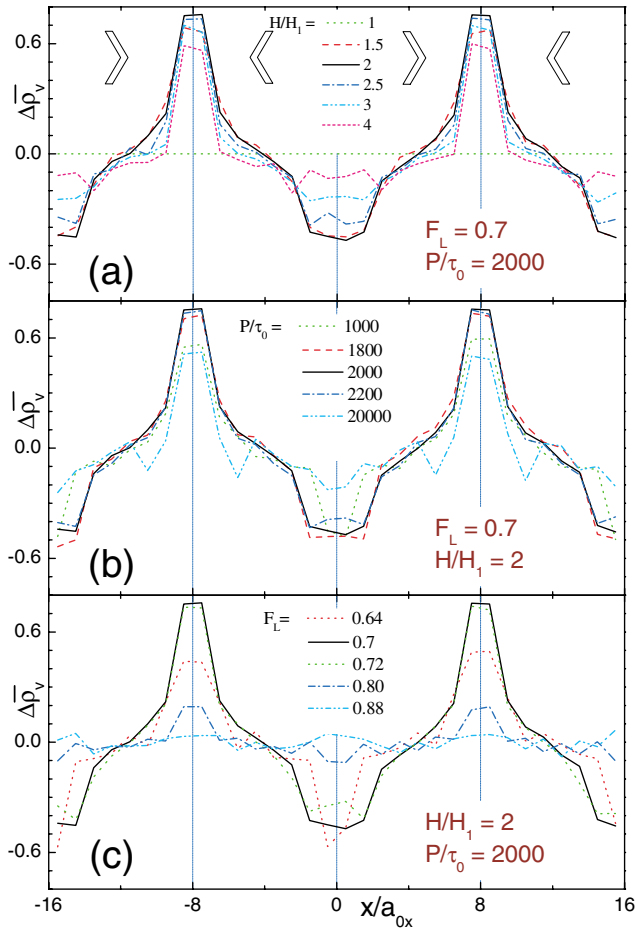

FIG. 4 (color). Subtracted average vortex density $\Delta\bar{\rho}_v(x)$, after a time of $100P$, for various (a) magnetic fields: $H/H_1 = 1$, 1.5, 2, 2.5, 3, and 4 at $P = 2000\tau_0$ and $F_L = 0.7$; (b) driving half periods: $P/\tau_0 = 1000$, 1800, 2000, 2200, and 20 000 at $H/H_1 = 2$ and $F_L = 0.7$; (c) ac driving forces: $F_L = 0.64$, 0.7, 0.72, 0.8, and 0.88 at $P = 2000\,\tau_0$ and $\bar{\rho}_0 = H/H_1 = 2$. Here, $a_{0x} = a_0 \sin(\alpha/2)$ and $N_p = 128 \times 4 = 512$.

vortices, thus causing a vortex current inversion for any $P > P_c$. Moreover, when F_L is so small that $P < P_c$, it may happen that in one half period P vortices moving forward cannot make it to the next boomerang site (located a distance $a_0\sqrt{3}$). Still, interstitial vortices moving backwards jump out of one side tip of the boomerang and get retrapped at the tip of the closest boomerang on the adjacent row (located a distance $a_0\sqrt{3}/2$). Thus, interstitial vortices are responsible also for the weak negative vortex flow in the subthreshold regime $0.5P_c < P < P_c$ of Fig. 1(a). Analytical results and vortex trajectory patterns will be shown elsewhere [10].

Magnetic lensing effect.—In Fig. 3, we show the "lensing effect" of vortices subject to an ac drive in a striped pinning structure made of *bras* $<$ and *kets* $>$, i.e., of chevrons or boomerangs pointing to the left $<$ and to the right $>$, respectively. We simulated four alternate stripes of *bras* and *kets*, each containing 128 pinning centers arranged on eight rows; the remaining geometric pinning parameters being as in Fig. 1. Figure 3 (top panel) shows a snapshot of the spatial distribution of the vortices after 50 drive cycles with $F_L = 0.7$ and $P = 2000\tau_0$; in Fig. 3 (lower panel) is the corresponding vortex density per pinning site $\rho_v(x)$ along the x axis: The lensing power of both the focusing and defocusing geometries is striking. Notice that the maximum vortex density (convex lens) is over significantly higher than the lowest vortex density (concave lens).

In Figs. 4(a)–4(c), we show the dependence of the time-averaged vortex density $\bar{\rho}_v(x)$ on the magnetic field H/H_1, and on the half period P and the amplitude F_L of the ac drive. Each curve in Figs. 4(a)–4(c) has been obtained by averaging the vortex distribution of 200 snapshots of the system taken half cycle apart, after a time of $100P$.

The excess vortices at the stripe interfaces are quantified by $\Delta\bar{\rho}_v(x) \equiv \bar{\rho}_v(x) - \bar{\rho}_0$, where $\bar{\rho}_0 = H/H_1$ is the expected vortex density per pinning site in the absence of external bias and $\int \Delta\bar{\rho}_v(x)dx = 0$. As shown in Fig. 4(c),the lensing effect is maximum for $F_L \simeq 0.7$, when the rectification effect of Fig. 2 is also the strongest; namely, adjacent pinning stripes tend to pump vortices towards the *ket-bra*, $> <$, interfaces (convex lens), due to ratchet mechanism. The ability of a $> <$ interface to pile up vortices is rather insensitive to the initial vortex density $\bar{\rho}_0$, thus implying a saturation effect for $H > H_1$ (at $H \leq H_1$, the lensing effect vanishes altogether as all vortices are pinned—no interstitials, there). For the optimal lensing configuration in Fig. 4(a), about two vortices per pinning sites ($H/H_1 \simeq 2$) get trapped at the $> <$ interfaces, although this number necessarily decreases in the adiabatic regime $P \gg P_c$; see Fig. 4(b).

We emphasize that, with modifications, these results also apply to arrays of Josephson junctions, colloidal systems, Wigner crystals and any system with repelling movable objects that can be pinned by asymmetric traps [11]. A recent example [12] illustrates how results from our previous predictions [13] can be extended to experiments on colloidal systems.

We acknowledge support from the Canon Foundation and the U.S. National Science Foundation Grant No. EIA-0130383.

*Permanent address.
Corresponding author.
Electronic address: nori@umich.edu

[1] R. D. Astumian and P. Hänggi, Phys. Today **55**, No. 11, 33 (2002); P. Reimann, Phys. Rep. **361**, 57 (2002); R. Eichhorn *et al.*, Phys. Rev. Lett. **88**, 190601 (2002); F. Jülicher *et al.*, Rev. Mod. Phys. **69**, 1269 (1997); R. D. Astumian, Science **276**, 917 (1997).

[2] R. Bartussek, P. Hänggi, and J. G. Kissner, Europhys. Lett. **28**, 459 (1994); F. Marchesoni, Phys. Rev. E **56**, 2492 (1997); Phys. Lett. A **237**, 126 (1998); M. Borromeo *et al.*, Phys. Rev. E **65**, 041110 (2002); C. R. Doering, Physica (Amsterdam) **254A**, 1 (1998); Nuovo Cimento Soc. Ital. Fis. **17D**, 685 (1995); C. R. Doering *et al.*, Chaos **8**, 643 (1998).

[3] See, e.g., the many reviews in Special issue on *Ratchets and Brownian Motors: Basics, Experiments and Applications*, edited by H. Linke [Appl. Phys. A **75**, No. 2 (2002)].

[4] J. F. Wambaugh *et al.*, Phys. Rev. Lett. **83**, 5106 (1999); C. J. Olson *et al.*, *ibid.* **87**, 177002 (2001); W. Kwok *et al.*, Physica (Amsterdam) **382C**, 137 (2002); C. S. Lee *et al.*, Nature (London) **400**, 337 (1999); S. Savelev and F. Nori, Nature Mater. **1**, 179 (2002); B. Y. Zhu *et al.*, Physica (Amsterdam) **388C**, 665 (2003); Physica (Amsterdam) **18E**, 318 (2003); **18E**, 322 (2003); twin boundaries can act as a flux-gradient-driven vortex diode: J. Groth *et al.*, Phys. Rev. Lett. **77**, 3625 (1996).

[5] B. Y. Zhu *et al.*, Phys. Rev. B **65**, 14514 (2003).

[6] *Applications of Superconductivity*, edited by H. Weinstock (Kluwer, Dordrecht, 1999); *SQUID Sensors*, edited by H. Weinstock (Kluwer, Dordrecht, 1996).

[7] I. Zapata *et al.*, Phys. Rev. Lett. **77**, 2292 (1996); I. Zapata *et al.*, Phys. Rev. Lett. **80**, 829 (1998); G. Carapella *et al.*, *ibid.* **87**, 077002 (2001); S. Weiss *et al.*, Europhys. Lett. **51**, 499 (2000); F. Falo *et al.*, *ibid.* **45**, 700 (1999); E. Goldobin *et al.*, Phys. Rev. E **63**, 031111 (2001); E. Trías *et al.*, *ibid.* **61**, 2257 (2000); J. B. Majer *et al.*, Phys. Rev. Lett. **90**, 056802 (2003).

[8] F. Nori, Science **278**, 1373 (1996); C. Reichhardt *et al.*, Phys. Rev. B **52**, 10 441 (1995); **53**, R8898 (1996); **54**, 16 108 (1996); **56**, 14 196 (1997); C. Reichhardt *et al.*, Phys. Rev. B **57**, 7937 (1998).

[9] C. Reichhardt *et al.*, Phys. Rev. Lett. **78**, 2648 (1997); Phys. Rev. B **58**, 6534 (1998).

[10] B. Y. Zhu, F. Marchesoni, and F. Nori (unpublished).

[11] Color figures related to this work, and color animations showing the vortex motion, can be found at http://www-personal.engin.umich.edu/nori/ket/

[12] P. T. Korda *et al.*, Phys. Rev. Lett. **89**, 128301 (2002); **11**, story 6, 13 September 2002.

[13] C. Reichhardt and F. Nori, Phys. Rev. Lett. **82**, 414 (1999).